*Korean J. Chem. Eng.*, 37(5), 905-910 (2020)
DOI: 10.1007/s11814-020-0488-3

pISSN: 0256-1115
eISSN: 1975-7220

# Improved impact strength of poly(lactic acid) by incorporating poly(butylene succinate) and silicon dioxide nanoparticles

**Fan-Long Jin*,†, Rong-Rong Hu**, and Soo-Jin Park***,†**

*Department of Polymer Materials, Jilin Institute of Chemical Technology, Jilin City 132022, P. R. China
**Zhu-Hai CosMX Battery Co., Ltd. Zhu-Hai City 519180, P. R. China
***Department of Chemistry, Inha University, Nam-gu, Incheon 22212, Korea
(*Received 25 July 2019 • accepted 9 January 2020*)

**Abstract**−The surface of silicon dioxide ($SiO_2$) nanoparticles was treated with oleic acid, and the resulting surface properties were characterized. Bio-based poly(lactic acid) (PLA)/poly(butylene succinate)/$SiO_2$ nanocomposites were fabricated via solution blending. The influence of the $SiO_2$ content on the thermal stability, flexural properties, impact strength, and morphology of the prepared nanocomposites was investigated using several techniques. The impact strength of the nanocomposites with surface treated $SiO_2$ (O-$SiO_2$) nanoparticles substantially increased with increasing O-$SiO_2$ content from 0 to 3 wt%. Scanning electron microscopy imaging revealed that the nanocomposites with O-$SiO_2$ nanoparticles exhibited numerous tortuous cracks and ridges, indicating ductile deformation prior to fracturing.

Keywords: Poly(lactic acid), Poly(butylene succinate), Silicon Dioxide, Surface Modification, Impact Strength

## INTRODUCTION

Traditional petroleum-based polymers, including polyethylene, poly(vinyl chloride), and acrylonitrile butadiene styrene, have been widely used in several industries. However, these polymers cannot be naturally decomposed, causing serious environmental pollution. Reducing this pollution, necessitates the development of biodegradable and renewable biopolymers to replace the previously listed non-degradable petroleum-based polymers [1-4].

Biopolymers are prepared from renewable resources, and poly(lactic acid) (PLA) is the most popular biodegradable aliphatic polyester. PLA exhibits excellent biodegradability, biocompatibility, and nontoxic properties, and is widely used in packaging, textiles, cutleries, and biomedical applications [5-11]. Although PLA exhibits moderate physical properties compared with other biopolymers, commercial applications are limited by its high production cost and brittle nature.

In general, PLA can be toughened by plasticization, copolymerization, blending, and compounding. In the blending method, PLA is mixed with a biodegradable polymer to improve toughness and maintain biodegradability [12-14]. Among biodegradable polymers, poly (butylene succinate) (PBS) is a biodegradable aliphatic polyester that is inexpensive, biodegradable, processable, thermally stable, and chemically resistant. PBS also exhibits a low glass transition temperature of −45 to −5 °C, imparting it with substantial flexibility [15-20].

In the compounding method, PLA is mixed with nano-sized particles to create new biopolymer composites that exhibit excellent characteristics, including high toughness, good stiffness, and a high heat distortion temperature. Commonly used nano-sized particles include clay, silicon dioxide ($SiO_2$) nanoparticles, nanocellulose, and carbon-based nanoparticles [14].

Recently, nanoparticles have been widely used as compatibilizers to enhance the interfacial interaction between polymer blends. Tan et al. [21] prepared PLA/PBS/organically modified clay nanocomposites via volume pulsating elongation flow. Their results showed that the clay mainly dispersed in PBS and located at the interface of PLA/PBS blends. The addition of clay suppressed the aggregation of PBS, resulting in a decrease of the PBS diameter in the PLA/PBS blends. Wu et al. [22] studied the effect of nitrogen-doped graphene (NG) on the morphology and properties of PBS/PLA blends. Their results indicated that the domain size of the dispersed PLA phase in PBS/PLA blends decreased upon the addition of NG, indicating a compatibilization effect of NG on the immiscible blends. Transition electron microscopy (TEM) micrographs showed that the NG mainly dispersed in the PBS matrix, whereas a small amount was located in the PLA phase.

In this study, bio-based PLA/PBS/$SiO_2$ nanocomposites were fabricated by solution blending. The surface of the $SiO_2$ nanoparticles was treated with oleic acid. The influence of the $SiO_2$ amount on the thermal and flexural properties, impact strength, and morphology of the composites was investigated by thermogravimetric analysis (TGA), mechanical testing, Izod impact testing, and field-emission scanning electron microscopy (FE-SEM).

## EXPERIMENTAL

### 1. Materials

PLA (4032 D, weight-average molecular weight of 100,000 g/mol) as the polymer matrix was obtained from NatureWorks Co., USA. PBS (weight-average molecular weight of 50,000) was supplied by Eko New Materials Co., Ltd. (USA). $SiO_2$ nanoparticles (AEROSIL

†To whom correspondence should be addressed.
E-mail: jinfanlong@163.com, sjpark@inha.ac.kr

200) with a specific surface area of 200 $m^2/g$ and an average particle size of 50 nm were purchased from Degussa (Germany) for use as a reinforcing agent. Oleic acid was supplied by Tianjin Damao Chemical Reagent Factory (China) and used to modify the $SiO_2$ nanoparticles. Dichloromethane was obtained from Zhangjiagang Free Trade Zone Vibration Good Trade Co., Ltd. (China) and used as a solvent.

**2. Surface Modification of $SiO_2$ Nanoparticles**

Oleic acid (2 g) was dissolved in deionized water (100 mL) and $SiO_2$ (20 g) was subsequently added to the oleic acid solution. Ammonia solution (0.1 mol/L) was added to adjust the pH of the solution in the range of 8-9, and the mixture was stirred continuously at 30 °C for 10 h. The surface-treated $SiO_2$ nanoparticles were obtained after filtering, washing, and drying. The oleic acid-treated $SiO_2$ was denoted as O-$SiO_2$.

**3. Sample Preparation**

The PLA/PBS/$SiO_2$ ratio was varied from 80/20/0 to 80/20/4. PLA, PBS, and $SiO_2$ were dried at 60 °C for 24 h before use. PLA, PBS, and $SiO_2$ were added to dichloromethane and mixed at 30 °C for 3 h. The dichloromethane was subsequently removed by heat treatment at 180 °C for 4 h. The mixture was then injected into a mold and compression-molded at 180 °C and 4 MPa.

**4. Characterization and Measurements**

The surface properties of the $SiO_2$ nanoparticles before and after surface treatment were investigated using X-ray photoelectron spectroscopy (XPS, Thermo scientific, K-Alpha). The thermal properties of the $SiO_2$ nanoparticles before and after surface treatment were evaluated by TGA (TA Instruments, Q50) from 30 to 800 °C at a heating rate of 10 °C/min under a nitrogen flow of 30 mL/min. The morphology of the $SiO_2$ nanoparticles before and after surface treatment was examined by FE-SEM (Hitachi, SU 8010) and field-emission-transmission electron microscopy (FE-TEM, JEOL, JEM2100).

The thermal properties of the PLA/PBS/$SiO_2$ nanocomposites were investigated by TGA (TA Instruments, Q50) from 30 to 500 °C at a heating rate of 10 °C/min under a nitrogen flow of 30 mL/min.

Flexural tests of the nanocomposites were carried out according to methodology specified in standard ASTM D790-86. The impact strength of the composites was measured using an Izod impact tester (TP04G-AS1) according to the GB/T 1843-2008 standard method.

The morphology of the nanocomposites after the impact strength tests was investigated by FE-SEM (Hitachi, SU 8010). The dispersion state of the $SiO_2$ nanoparticles in PLA/PBS/$SiO_2$ nanocomposites was examined by FE-TEM (JEOL, JEM2100).

## RESULTS AND DISCUSSION

**1. Surface Modification of the $SiO_2$ Nanoparticles**

Fig. 1 shows the XPS spectra of the $SiO_2$ nanoparticles before and after surface treatment. The characteristic peak of O1s, which was observed at 533.8 eV, decreased substantially in intensity after the surface treatment with oleic acid. This decrease in intensity is attributed to the hydroxyl group on the $SiO_2$ surfaces reacting with oleic acid during the surface treatment [23,24].

Fig. 2 shows the TGA thermograms of the $SiO_2$ nanoparticles before and after the surface treatment. The weight loss at 800 °C

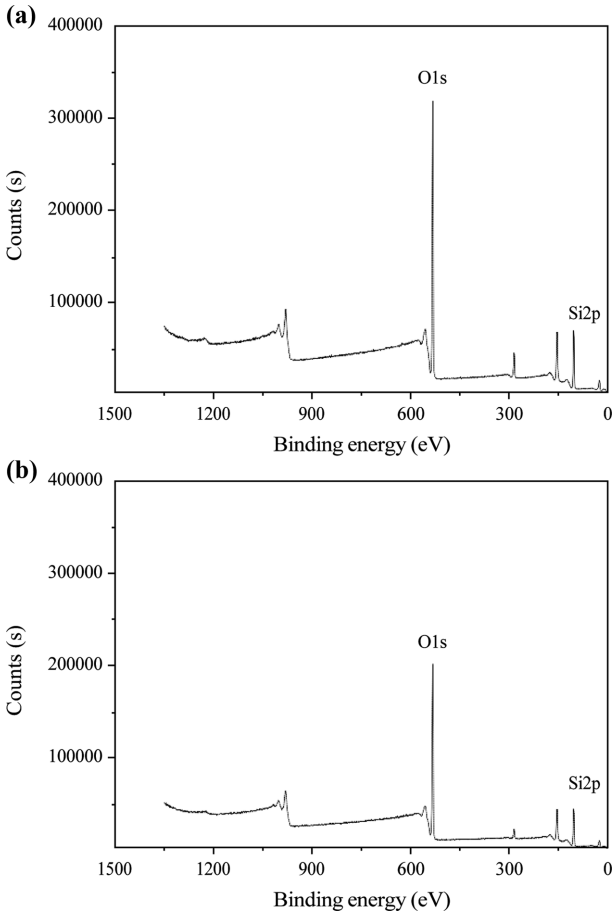


**Fig. 1. XPS spectra of $SiO_2$ nanoparticles (a) before and (b) after surface modification.**

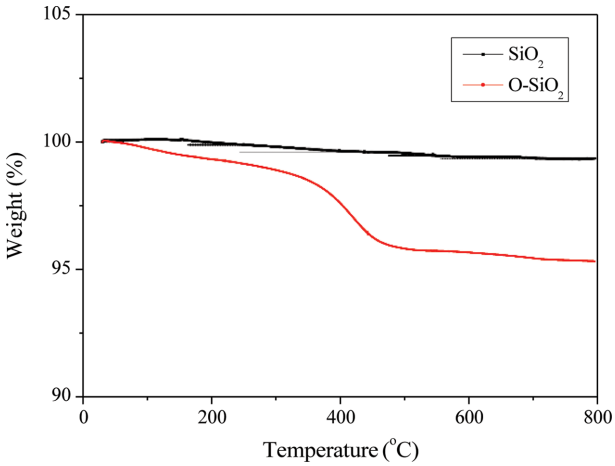


**Fig. 2. TGA thermograms of $SiO_2$ nanoparticles (a) before and (b) after surface modification.**

was calculated to be 0.64 and 4.66 wt% for the $SiO_2$ nanoparticles before and after surface treatment, respectively. These results indicate that the oleic acid content on the surface of O-$SiO_2$ was approximately 4 wt% [25,26].

The morphology of the $SiO_2$ nanoparticles before and after surface treatment was observed by SEM and TEM; the correspond-

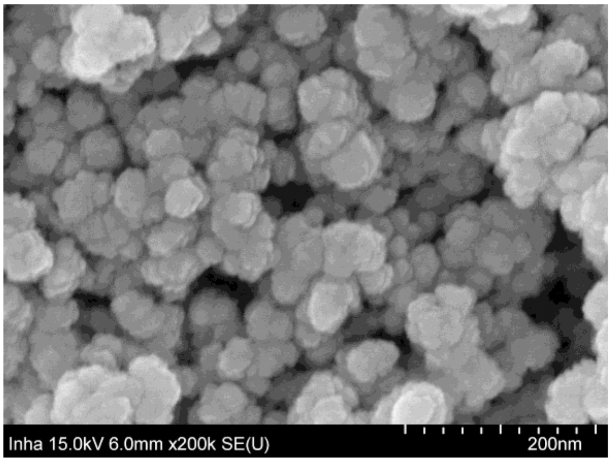


(a)

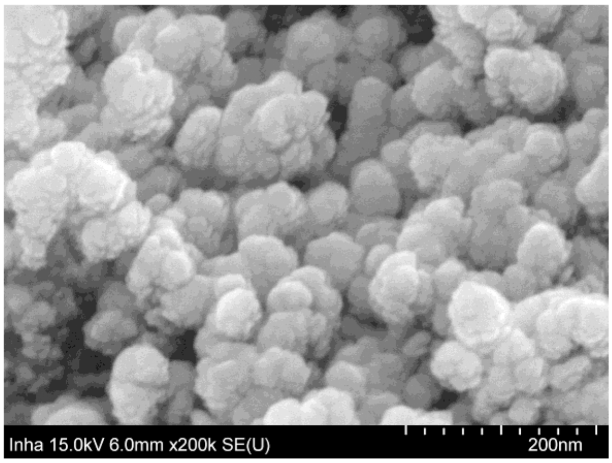


(b)

**Fig. 3. SEM micrographs of $SiO_2$ nanoparticles (a) before and (b) after surface modification (magnification of 200,000).**

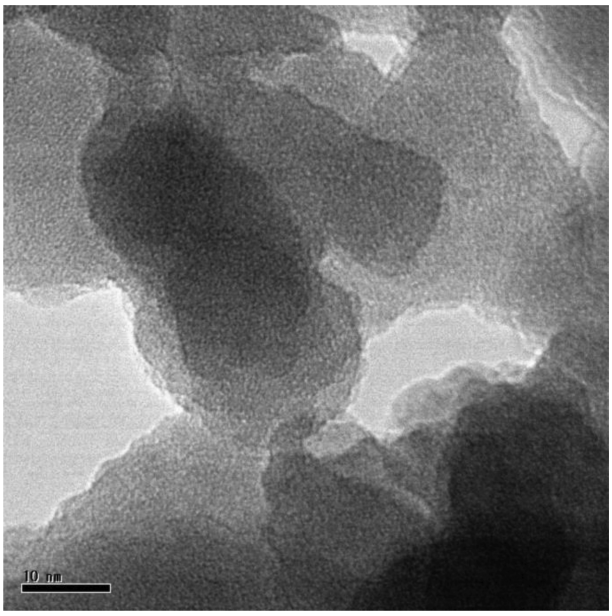


**Fig. 4. TEM image of O-$SiO_2$ nanoparticles.**

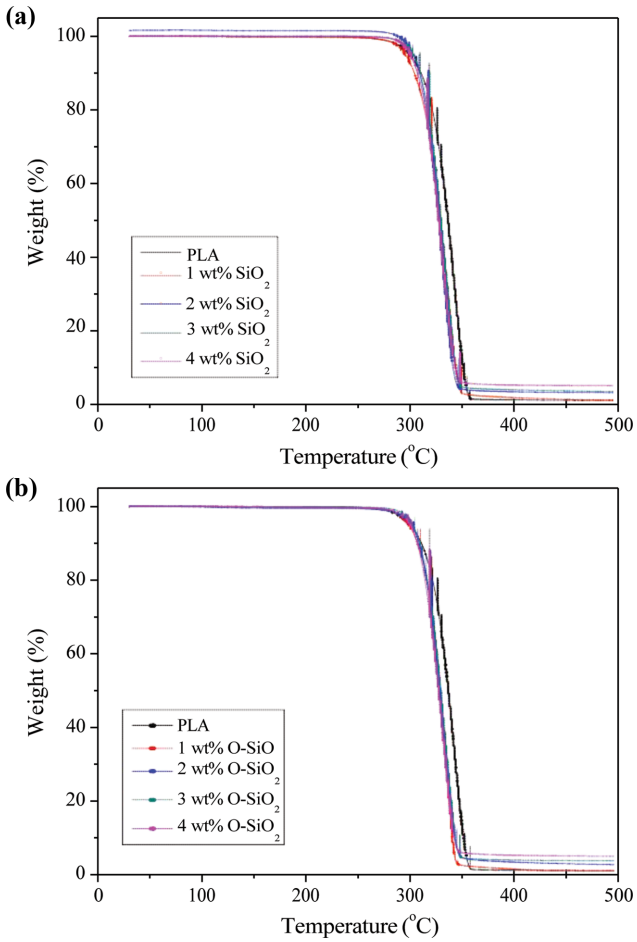


**Fig. 5. TGA thermograms of PLA/PBS/$SiO_2$ nanocomposites as a function of $SiO_2$ content.**

ing images are shown in Figs. 3 and 4, respectively. After surface treatment, the surface of the O-$SiO_2$ nanoparticles was coated with a thin layer compared with that of the pristine $SiO_2$ nanoparticles, indicating the attachment of organic moieties on the $SiO_2$ surfaces [26,27]. Thus, surface treatment with oleic acid introduced organic functional groups onto the surface of the $SiO_2$ nanoparticles.

**2. Thermal Properties of the PLA/PBS/$SiO_2$ Nanocomposites**

Fig. 5 shows the thermal properties of the PLA/PBS/$SiO_2$ nanocomposites. The thermal stability factors, including the decomposition temperature ($T_{5\%}$) for weight loss of 5% and char at 500 °C, were calculated from the TGA thermograms [28-30]; the results are summarized in Table 1. The $T_{5\%}$ value of the nanocomposite was similar to that of the neat PLA. The char value of the nanocomposites at 500 °C increased with increasing $SiO_2$ content. These results indicate that the introduction of the $SiO_2$ nanoparticles did not affect the thermal stability of the PLA polymer.

**3. Flexural Properties of the PLA/PBS/$SiO_2$ Nanocomposites**

The mechanical properties of the PLA/PBS/$SiO_2$ nanocomposites were studied using flexural strength and elastic modulus measurements. Fig. 6 shows the flexural strength of the PLA/PBS/$SiO_2$ nanocomposites. The flexural strength of the nanocomposites containing pristine $SiO_2$ nanoparticles decreased significantly from 122.7 to 81.4 MPa with increase in $SiO_2$ content from 0 to 4 wt%.

**Table 1. Thermal stability factors of PLA/PBS/$SiO_2$ nanocomposites obtained from TGA thermograms**

| PBS content (wt%) | $SiO_2$ content (wt%) | O-$SiO_2$ content (wt%) | T5% (°C) | Char at 500 °C (%) |
|---|---|---|---|---|
| 0 | 0 | 0 | 300.1 | 1.24 |
| 20 | 1 | 0 | 300.8 | 1.33 |
| 20 | 2 | 0 | 300.9 | 3.39 |
| 20 | 3 | 0 | 303.2 | 3.63 |
| 20 | 4 | 0 | 300.5 | 5.26 |
| 20 | 0 | 1 | 298.6 | 1.17 |
| 20 | 0 | 2 | 300.8 | 2.90 |
| 20 | 0 | 3 | 302.8 | 3.95 |
| 20 | 0 | 4 | 300.0 | 5.18 |

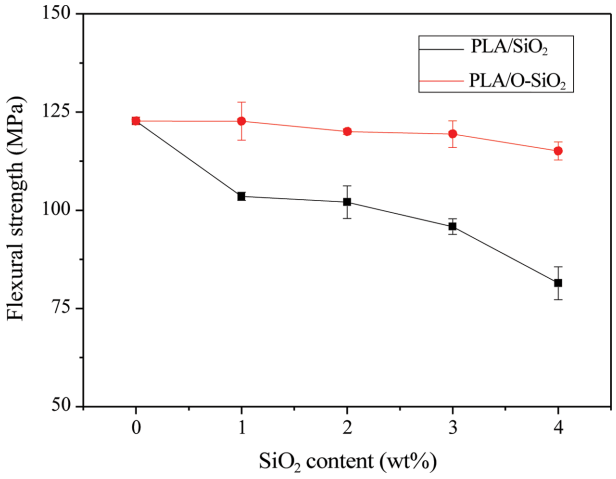


**Fig. 6. Flexural strength of PLA/PBS/$SiO_2$ nanocomposites as a function of $SiO_2$ content.**

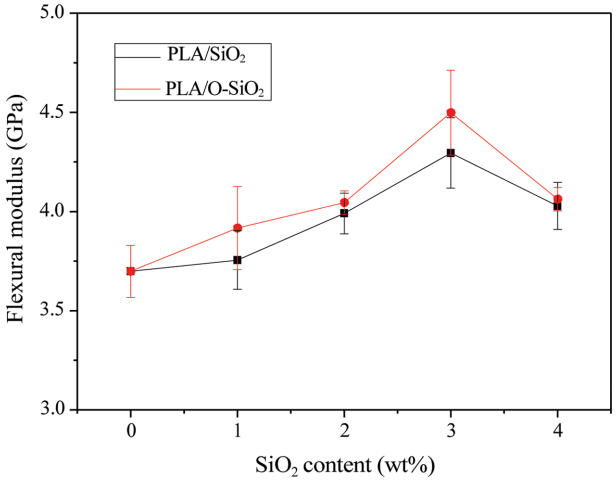


**Fig. 7. Elastic modulus of PLA/PBS/$SiO_2$ nanocomposites as a function of $SiO_2$ content.**

However, the flexural strength of the nanocomposites containing O-$SiO_2$ nanoparticles only slightly decreased from 122.7 to 115.1 MPa when the O-$SiO_2$ content increased. This is attributed to the improved interfacial adhesion between the O-$SiO_2$ nanoparticles and PLA matrix in the PLA/$SiO_2$ nanocomposites [31,32].

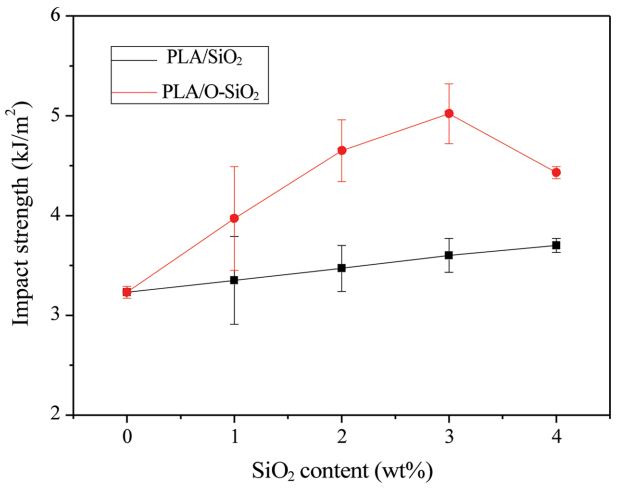


**Fig. 8. Impact strength of PLA/PBS/$SiO_2$ nanocomposites as a function of $SiO_2$ content.**

Fig. 7 shows the elastic modulus of the PLA/PBS/$SiO_2$ nanocomposites. The elastic moduli of the nanocomposites with pristine $SiO_2$ and O-$SiO_2$ nanoparticles increased with increasing $SiO_2$ content from 0 to 3 wt%. The elastic moduli of the PLA/PBS/$SiO_2$ nanocomposites with pristine $SiO_2$ and O-$SiO_2$ nanoparticles were 4.3 and 4.5 GPa, which are 16% and 22% higher than that of pristine PLA, respectively.

## 4. Impact Strength of the PLA/PBS/$SiO_2$ Nanocomposites

Fig. 8 shows the impact strength of the PLA/PBS/$SiO_2$ nanocomposites. The impact strength of the nanocomposites containing pristine $SiO_2$ nanoparticles increased slightly from 3.2 to 3.7 kJ/$m^2$ with increasing $SiO_2$ content from 0 to 4 wt%. The impact strength of the nanocomposites containing O-$SiO_2$ nanoparticles significantly increased from 3.2 to 5 kJ/$m^2$ when the O-$SiO_2$ content was increased from 0 to 3 wt%, resulting in a 56% increase over that of the pristine PLA and a 35% increase over that of the nanocomposites with neat $SiO_2$ nanoparticles. This result is attributed to the O-$SiO_2$ nanoparticles functioning as a compatibilizer and improving the interfacial interaction between the PLA and PBS polymers [21,22]. The increase in impact strength was also due to numerous cracks created in the PLA matrix by the $SiO_2$ nanoparticles, which enabled the absorption of more external energy [33,34].

The impact strength of the nanocomposites containing O-$SiO_2$

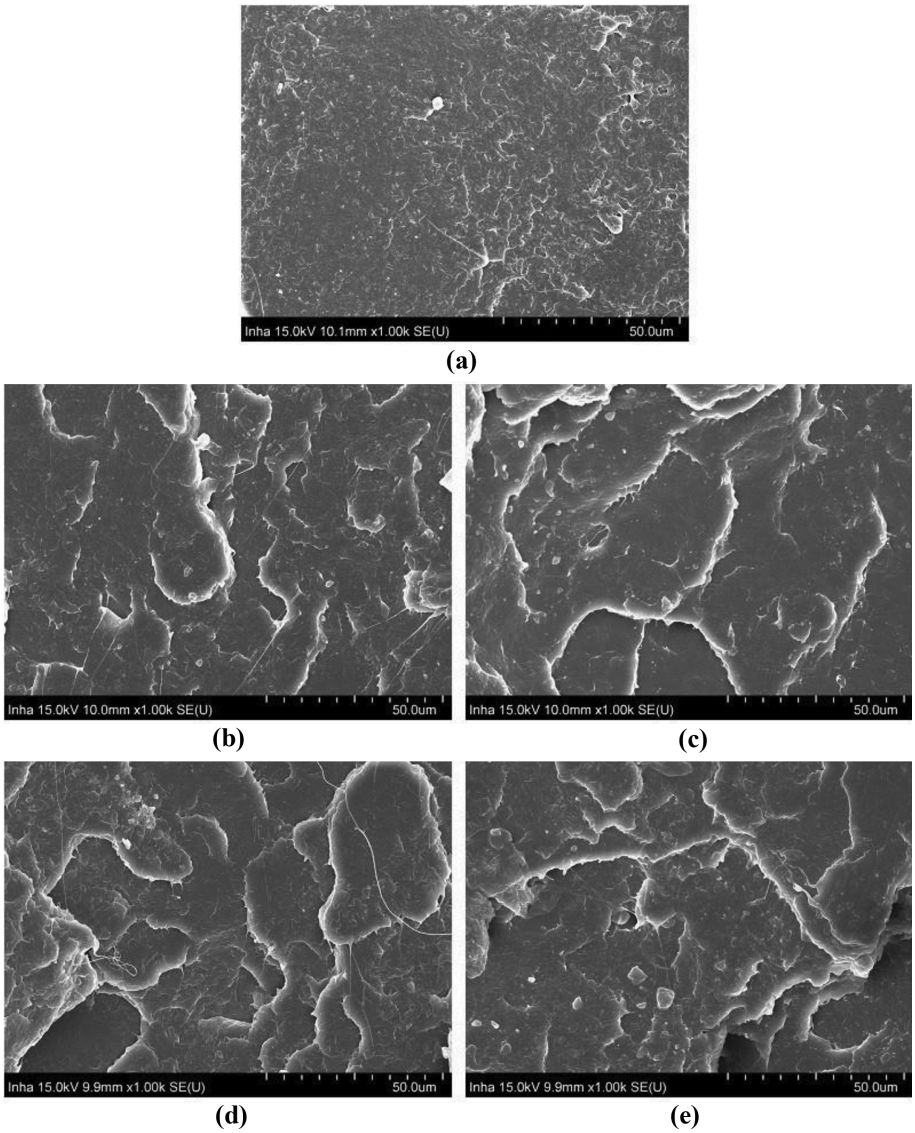


**Fig. 9. SEM micrographs of PLA/PBS/$SiO_2$ nanocomposites after impact strength tests: (a) Pristine PLA; (b) 1 wt% $SiO_2$; (c) 3 wt% $SiO_2$; (d) 1 wt% O-$SiO_2$; (e) 3 wt% O-$SiO_2$ (magnification of 1,000).**

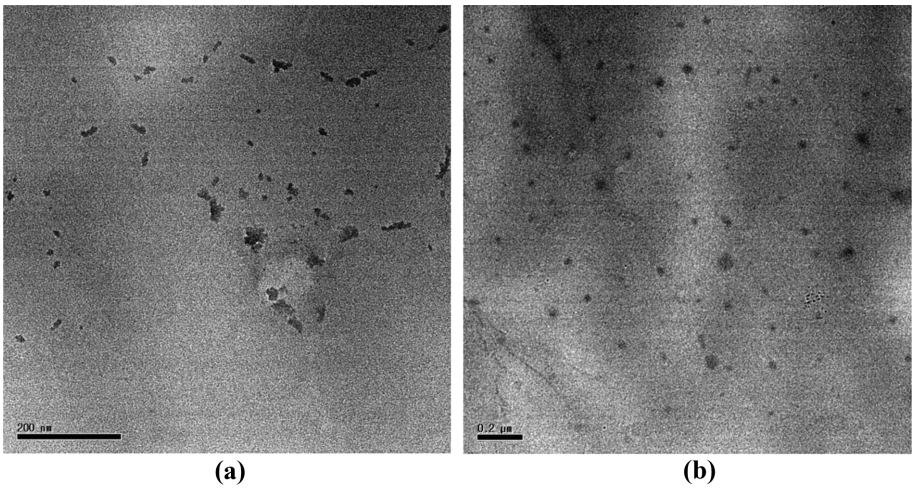


**Fig. 10. TEM images of PLA/PBS/$SiO_2$ nanocomposites: (a) Aggregated $SiO_2$ nanoparticles; (b) well distributed O-$SiO_2$ nanoparticles.**

nanoparticles slightly decreased when the O-$SiO_2$ content increased from 3 to 4 wt%. This result is attributed to the O-$SiO_2$ nanoparticles aggregating at high O-$SiO_2$ contents.

**5. Morphology of the PLA/PBS/$SiO_2$ Nanocomposites**

The toughness behavior of the PLA/PBS/$SiO_2$ nanocomposites was further characterized by SEM. Fig. 9 shows SEM images of the PLA/PBS/$SiO_2$ nanocomposites after the impact strength tests. As shown in Fig. 9(a), the neat PLA exhibits a flattened morphology, indicating a brittle fracture surface [35]. By contrast, the SEM images of the nanocomposites with pristine $SiO_2$ nanoparticles show a rough morphology, indicating ductile deformation prior to fracturing (Figs. 9(b) and (c)). The SEM images of the nanocomposites with O-$SiO_2$ nanoparticles show numerous tortuous cracks and ridges, indicating ductile deformation prior to fracturing (Figs. 9(d) and (e)) [34,36], accounting for the high impact strength of the PLA/PBS/$SiO_2$ nanocomposites.

The dispersion state of the $SiO_2$ nanoparticles in the PLA/PBS/$SiO_2$ nanocomposites was examined by TEM; the corresponding micrographs of the nanocomposites are shown in Fig. 10. As shown in Fig. 10(a), the $SiO_2$ nanoparticles are aggregated in the nanocomposites. After the surface modification, $SiO_2$ nanoparticles were well distributed in the nanocomposites, as shown in Fig. 10(b).

## CONCLUSIONS

The thermal and flexural properties, impact strength, and morphology of the PLA/PBS/$SiO_2$ nanocomposites were examined. The thermal stability of the nanocomposite was similar to that of the neat PLA. The flexural strength of the nanocomposites slightly decreased after the surface treatment of the $SiO_2$ nanoparticles. The nanocomposites showed a maximum value of elastic modulus at 3 wt% $SiO_2$. The impact strength of the nanocomposites containing O-$SiO_2$ nanoparticles substantially increased with increasing O-$SiO_2$ content from 0 to 3 wt%, reaching a value 56% greater than that of the neat PLA and 35% greater than that of the nanocomposites containing pristine $SiO_2$ nanoparticles. The results indicate that improved impact strength of PLA was achieved without sacrificing the thermal and mechanical properties of the nanocomposites.

## ACKNOWLEDGEMENTS

This work was supported by the Technology Innovation Program (or Industrial Strategic Technology Development Program (10083586, Development of petroleum based graphite fibers with ultra-high thermal conductivity) funded by the Ministry of Trade, Industry & Energy (MOTIE, Korea) and the Technological Innovation R&D Program (S2829590) funded by the Small and Medium Business Administration (SMBA, Korea).

## REFERENCES

1. F. L. Jin, R. R. Hu and S. J. Park, *Compos. Part B*, **164**, 287 (2019).
2. N. Wu, J. Yu, W. Lang, X. Ma and Y. Yang, *Polymers*, **11**(7), 1129 (2019).
3. J. Andrzejewski, M. Szostak, M. Barczewski and P. Łuczak, *Compos. Part B*, **163**, 655 (2019).
4. S. W. Kim and H. M. Choi, *Korean J. Chem. Eng.*, **33**(1), 330 (2016).
5. S. Liu, G. Wu, X. Chen, X. Zhang, J. Yu, M. Liu, Y. Zhang and P. Wang, *Polymers*, **11**(6), 1015 (2019).
6. M. K. Lila, K. Shukla, U. K. Komal and I. Singh, *Compos. Part B*, **156**, 121 (2019).
7. Y. Zhao, Y. Zhang, Z. Li, H. Pan, Q. Dong, L. Han, H. Zhang and L. Dong, *Korean J. Chem. Eng.*, **33**(3), 1104 (2016).
8. C. Vasile, E. Stoleru, R. N. Darie-Niţa, R. P. Dumitriu, D. Pamfil and L. Tarţau, *Polymers*, **11**(6), 941 (2019).
9. J. Li, W. J. Peng, Z. J. Fu, X. H. Tang, H. Wu, S. Guo and M. Wang, *Compos. Part B*, **171**, 204 (2019).
10. A. Lopera-Valle, J. V. Caputo, R. Leão, D. Sauvageau, S. M. Luz and A. Elias, *Polymers*, **11**(6), 933 (2019).
11. A. Djukić-Vuković, D. Mladenović, J. Ivanović, J. Pejin and L. Mojović, *Renew. Sust. Energy Rev.*, **108**, 238 (2019).
12. A. L. Hou and J. P. Qu, *Polymers*, **11**(5), 771 (2019).
13. M. Perić, R. Putz and C. Paulik, *Eur. Polym. J.*, **114**, 426 (2019).
14. B. Dillon, P. Doran, E. Fuenmayor, A. V. Healy, N. M. Gately, I. Major and J. G. Lyons, *Polymers*, **11**(4), 710 (2019).
15. M. Nofar, D. Sacligil, P. J. Carreau, M. R. Kamal and M. C. Heuze, *Int. J. Biol. Macromol.*, **125**, 307 (2019).
16. A. F. Ahmad, S. A. Aziz, Z. Abbas, S. J. Obaiys, K. A. Matori, M. H. M. Zaid, H. K. Raad and U. S. Aliyu, *Polymers*, **11**(4), 661 (2019).
17. J. Sun, L. Li and J. Li, *Chem. Eng. J.*, **369**, 150 (2019).
18. R. Liu, X. Yin, A. Huang, C. Wang and E. Ma, *Polymers*, **11**(2), 204 (2019).
19. T. M. Don, T. S. Li and W. C. Lai, *Polym. Degrad. Stab.*, **162**, 55 (2019).
20. M. J. Kang, F. L. Jin and S. J. Park, *Macromol. Res.*, **26**(11), 1048 (2018).
21. L. Tan, Y. He and J. Qu, *Polymer*, **180**, 121656 (2019).
22. W. Wu, C. Wu, H. Peng, Q. Sun, L. Zhou, J. Zhuang, X. Cao, V. A. L. Roy and R. K. Y. Li, *Compos. Part B*, **113**, 300 (2017).
23. S. J. Park and B. J. Kim, *Mater. Sci. Eng. A*, **408**(1-2), 269 (2005).
24. I. Jang, K. H. Shin, I. Yang, H. Kim, J. Kim, W. H. Kim, S. W. Jeon and J. P. Kim, *Colloids Surf. A*, **18**, 64 (2017).
25. F. L. Jin, H. Zhang, S. S. Yao and S. J. Park, *Macromol. Res.*, **26**(3), 211 (2018).
26. C. Pan, K. Kou, Q. Jia, Y. Zhang, G. Wu and T. Ji, *Compos. Part B*, **111**, 83 (2017).
27. F. L. Jin, C. J. Ma and S. J. Park, *Mater. Sci. Eng. A*, **528**(29-30), 8517 (2011).
28. F. L. Jin and S. J. Park, *Polym. Degrad. Stab.*, **97**(11), 2148 (2012).
29. F. L. Jin and S. J. Park, *Mater. Sci. Eng. A*, **475**(1-2), 190 (2008).
30. S. S. Yao, Q. Q. Pang, R. Song, F. L. Jin and S. J. Park, *Macromol. Res.*, **24**(11), 961 (2016).
31. F. L. Jin, Q. Q. Pang, T. Y. Zhang and S. J. Park, *J. Ind. Eng. Chem.*, **32**, 77 (2015).
32. J. H. Wu, M. S. Yen, M. C. Kuo and B. H. Chen, *Mater. Chem. Phys.*, **142**(2-3), 726 (2013).
33. F. L. Jin and S. J. Park, *Polym. Degrad. Stab.*, **92**(3), 509 (2007).
34. M. Foruzanmehr, P. Y. Vuillaume, S. Elkoun and M. Robert, *Mater. Des.*, **106**, 295 (2016).
35. Z. Li, J. K. Muiruri, W. Thitsartarn, X. Zhang, B. H. Tan and C. He, *Compos. Sci. Technol.*, **159**, 11 (2018).
36. J.B. Zhang, H. Zhang, F. L. Jin and S. J. Park, *B. Mater. Sci.*, **43**, 6 (2020).